Orbital Diamagnetism of Weak-doped Bilayer Graphene in Magnetic Field

Min Lv and Shaolong Wan*

Institute for Theoretical Physics and Department of Modern Physics
University of Science and Technology of China, Hefei, 230026, **P. R. China**

(Dated: January 10, 2011)

We investigate the orbital diamagnetism of a weak-doped bilayer graphene (BLG) in spatially smoothly varying magnetic field and obtain the general analytic expression of the orbital susceptibility of BLG, with finite wave number and Fermi energy, at zero temperature. We find that the magnetic field screening factor of BLG is dependent with the wave number, which results in a more complicated screening behavior compared with that of monolayer graphene (MLG). We also study the induced magnetization, electric current in BLG, under nonuniform magnetic field, and find that they are qualitatively different from that in MLG and two-dimensional electron gas (2DEG). However, similar to the MLG, the magnetic object placed above BLG is repelled by a diamagnetic force from BLG, approximately equivalent to a force produced by its mirror image on the other side of BLG with a reduced amplitude dependent with the typical length of the systems. BLG shows crossover behaviors in the responses to the external magnetic field as the intermediate between MLG and 2DEG.

PACS numbers: 75.20.-g, 73.63.-b, 75.70.Cn, 81.05.Uw

1. INTRODUCTION

Bilayer graphene (BLG), as a significant graphene-related material, has attracted much attentions [1–3] due to its unusual electronic structure. Formed by stacking two monolayer graphene (MLG) in Bernal stacking, Bilayer graphene has four inequivalent sites in each unit cell, including A_1 and B_1 atoms on the top layer and A_2 and B_2 atoms on the bottom layer. The distance a between A_1 and B_1 is about 0.142 nm and the vertical separation of the two layers d is about 0.334 nm. On its band structure side, around the point where the conduction and valence band touch, BLG has a quadratic energy dispersion [1] similar to the regular two-dimensional electron gas (2DEG) but its low-energy effective Hamiltonian is chiral without bandgap similar to the MLG. Another unique feature of BLG is that a widely tunable bandgap can realize conveniently by introducing an electrostatic potential bias between the up and bottom layer [1, 4–8].

The magnetic susceptibility of electronic systems comes from two contribution: One is Pauli paramagnetism which stems from spin polarization; The other is Landau diamagnetism which stems from the circulation of orbital currents. The orbital diamagnetism of carbon systems has attracted the interest of both experimental and theoretical physicists for a long time. It was firstly found by Krishnan [9] that the diamagnetic susceptibility of the bulk graphite is large and anisotropic. McClure [10] showed it arises from the Landau quantization of 2D massless Dirac fermions, which results in a delta function peak at zero energy in the orbital diamagnetism of graphite. After the experimentally fabrication of graphene, a great deal of works have concerned about the orbital magnetism of graphene-related systems, such as nodal fermions [11], disordered graphene [12–14], few-layered graphene [15–17], graphene in nonuniform magnetic field [18, 19]. Quite recently, novel paramagnetic susceptibility has been found in MLG and BLG with bandgap [20] and doped graphene to the first order in the Coulomb interaction [21].

Safran [22], Koshino and Ando [15] have derived the analytical expression of orbital susceptibility $\chi(0)$ for bilayer graphene, but their results are just limited to the case of zero wave number. In this article we generalize them to general cases and analytically study the orbital diamagnetism of a weak-doped BLG (i.e., the Fermi energy ϵ_F is much smaller than the interlayer hopping energy.) in nonuniform magnetic fields.

This article is organized as follows. In Sec. II, the effective Hamiltonian of bilayer graphene and its corresponding eigenstates and eigenenergies are introduced. In Sec. III, the orbital susceptibility of bilayer graphene is studied. In Sec. IV, we investigate and discuss the responses of bilayer graphene to several specific external magnetic field. The conclusion is given in Sec. V.

*Corresponding author; Electronic address: slwan@ustc.edu.cn

2. BILAYER GRAPHENE EFFECTIVE MODEL

In the low energy and long wave regime, the BLG Hamiltonian near a K point, in the absence of a magnetic field, can written as an excellent approximate form [1] (we set $c = 1 = \hbar$ in this paper):

$$H_0 = \begin{pmatrix} 0 & \gamma\hat{k}_- & 0 & 0 \\ \gamma\hat{k}_+ & 0 & \Delta & 0 \\ 0 & \Delta & 0 & \gamma\hat{k}_- \\ 0 & 0 & \gamma\hat{k}_+ & 0 \end{pmatrix}, \tag{1}$$

where $\gamma = 3ta/2 \approx 10^6 m/s$ is the monolayer graphene Fermi velocity, $t \approx 3eV$ is the in-plane hopping energy, $a \approx 0.142$ nm is the in-plane interatomic distance, $\Delta \approx 0.35eV$ is the interlayer hopping energy. $\hat{\boldsymbol{k}} = (\hat{k}_x, \hat{k}_y) = -i\boldsymbol{\nabla}$ is a 2D wave-vector operator, $\hat{k}_\pm = \hat{k}_x \pm i\hat{k}_y$. In order to solve the eigen equation of the Hamiltonian (1), the wave function can be expressed as $(\psi_{A_1}, \psi_{B_1}, \psi_{A_2}, \psi_{B_2})$, where the four components represent the Bloch functions at A_1, B_1, A_2 and B_2 sites, respectively. Follow the stipulation of Ando [23], and define

$$\epsilon(k) = \sqrt{(\frac{\Delta}{2})^2 + (\gamma k)^2}, \tag{2}$$

$$\gamma k = \epsilon(k)\sin\psi, \tag{3}$$

$$\frac{\Delta}{2} = \epsilon(k)\cos\psi. \tag{4}$$

Then the corresponding eigenstates of Eq.(1) are given as

$$\Psi_{sj\boldsymbol{k}}(\boldsymbol{r}) = \frac{1}{L}\exp(i\boldsymbol{k}\cdot\boldsymbol{r})U[\theta_{\boldsymbol{k}}]F_{sjk}, \tag{5}$$

where L^2 is the area of the system, $s = +1$ and -1 denote the conduction and valence bands, respectively, $j = 1$ and 2 specifies two subbands within the conduction or valence bands, $\theta_{\boldsymbol{k}} = \arctan(k_y/k_x)$ is the polar angle of the momentum $\boldsymbol{k}$,

$$U(\theta) = \begin{pmatrix} 1 & 0 & 0 & 0 \\ 0 & e^{i\theta} & 0 & 0 \\ 0 & 0 & e^{i\theta} & 0 \\ 0 & 0 & 0 & e^{2i\theta} \end{pmatrix}, \tag{6}$$

and

$$F_{s1k} = \frac{1}{\sqrt{2}}\begin{pmatrix} s\cos(\psi/2) \\ \sin(\psi/2) \\ -s\sin(\psi/2) \\ -\cos(\psi/2) \end{pmatrix}, \qquad F_{s2k} = \frac{1}{\sqrt{2}}\begin{pmatrix} s\sin(\psi/2) \\ \cos(\psi/2) \\ s\cos(\psi/2) \\ \sin(\psi/2) \end{pmatrix}. \tag{7}$$

The corresponding eigenenergies of Eq.(1) are

$$\begin{aligned} \epsilon_{s1}(k) &= 2s\epsilon(k)\sin^2(\psi/2), \\ \epsilon_{s2}(k) &= 2s\epsilon(k)\cos^2(\psi/2). \end{aligned} \tag{8}$$

Considering a magnetic field $\boldsymbol{B}(\boldsymbol{r}) = [\nabla \times \boldsymbol{A}(\boldsymbol{r})]_z$, the Hamiltonian for the system is: $H = H_0 + H_1$, with $H_1 = -\int d^2 r j_\alpha(\boldsymbol{r}) A_\alpha(\boldsymbol{r}, t)$. The current operator at $\boldsymbol{r}_0$ is given

$$\hat{j}_\alpha(\boldsymbol{r_0}) = \frac{e}{2}[\hat{v}_\alpha \delta(\boldsymbol{r} - \boldsymbol{r}_0) + \delta(\boldsymbol{r} - \boldsymbol{r}_0)\hat{v}_\alpha], \qquad (\alpha = x, y) \tag{9}$$

where $\hat{v}_\alpha$ is velocity operator

$$\hat{v}_\alpha = \frac{\partial H_0}{\partial k_\alpha} = \gamma \begin{pmatrix} \sigma_\alpha & 0 \\ 0 & \sigma_\alpha \end{pmatrix}, \qquad (\alpha = x, y) \tag{10}$$

$\sigma_{x,y}$ are the Pauli matrices which act on the sublattice space within a layer.

3. ORBITAL SUSCEPTIBILITY

The finite wave number susceptibility $\chi(\boldsymbol{q})$ can be obtained through the Kubo formula [24]. Within the linear response theory, the external vector potential $\boldsymbol{A}$ and the its induced 2D electric current density $\boldsymbol{j}$ have a relation

$$j_\mu(\boldsymbol{q}) = \sum_\nu K_{\mu\nu}(\boldsymbol{q}) A_\nu(\boldsymbol{q}), \tag{11}$$

and the orbital susceptibility $\chi(\boldsymbol{q})$ and the response tensor $K_{\mu\nu}(\boldsymbol{q})$ are related by

$$K_{\mu\nu}(\boldsymbol{q}) = q^2 \chi(\boldsymbol{q})(\delta_{\mu\nu} - \frac{q_\mu q_\nu}{q^2}). \tag{12}$$

In the first order perturbation, we have

$$K_{\mu\nu}(\boldsymbol{q}) = -\frac{g}{L^2} \sum_{ss'jj'\boldsymbol{k}} \frac{f[\epsilon_{sj}(k)] - f[\epsilon_{s'j'}(k')]}{\epsilon_{sj}(k) - \epsilon_{s'j'}(k')} I_{ss',jj'}, \tag{13}$$

where $g = g_v g_s = 4$ is the total degeneracy, $\boldsymbol{k'} = \boldsymbol{k} + \boldsymbol{q}$, $\epsilon_{sj}(k)$ is the eigenenergy given by Eq.(8), $f(\epsilon)$ is the Fermi distribution function $f(\epsilon) = [1 + \exp\beta(\epsilon - \epsilon_F)]^{-1}$ where ϵ_F is the Fermi energy, $\beta = 1/(k_B T)$. $I_{ss',jj'}$ is the current-current response matrix element expressed by

$$I_{ss',jj'} = \left[F^\dagger_{s'j'\boldsymbol{k'}} U^\dagger(\theta_{\boldsymbol{k'}}) v_\mu U(\theta_{\boldsymbol{k}}) F_{sj\boldsymbol{k}}\right] \left[F^\dagger_{sj\boldsymbol{k}} U^\dagger(\theta_{\boldsymbol{k}}) v_\nu U(\theta_{\boldsymbol{k'}}) F_{s'j'\boldsymbol{k'}}\right], \tag{14}$$

which determines the weight of contribution of the transition from subband j to j', with $ss' = +1$ and -1 denote the intraband and interband transition, respectively.

Define the effective mass $m \equiv \Delta/(2\gamma^2) \approx 0.033 m_e$ and the Fermi wave number $k_F \equiv \sqrt{2m\epsilon_F}$. For a low-energy theory of bilayer graphene, there is a natural high-energy cutoff wave number $\Lambda \equiv \sqrt{2m\Delta} = \Delta/\gamma$. When $k_F, q \ll \Lambda$, i.e., when bilayer graphene is weak-doped and the external field is smooth enough compared to the cutoff wavelength, the transitions intra the same j subband dominate the contribution to the response function. One of these transitions is the transition intra the $j = 1$ subband:

$$K_{\mu\nu,11}(\boldsymbol{q}) = -\frac{g}{L^2} \sum_{ss'\boldsymbol{k}} \frac{f[\epsilon_{s1}(k)] - f[\epsilon_{s'1}(k')]}{\epsilon_{s1}(k) - \epsilon_{s'1}(k')} I_{ss',11}. \tag{15}$$

In the low energy limit, it can be approximately given as

$$K_{\mu\nu,11}(\boldsymbol{q}) \approx -\frac{ge^2}{m^2 L^2} \sum_{ss'\boldsymbol{k}} \frac{f[s\epsilon_k] - f[s'\epsilon_{k'}]}{s\epsilon_k - s'\epsilon_{k'}} \left[\frac{1}{2}(\boldsymbol{k} + \frac{\boldsymbol{q}}{2})^2 \delta_{\mu\nu} + \frac{ss'}{8} F_{\mu\nu}\right], \tag{16}$$

with $\epsilon_k = k^2/(2m)$ and

$$\begin{aligned} F_{\mu\nu} = &(\delta_{\mu1}\delta_{\nu1} - \delta_{\mu2}\delta_{\nu2}) \left[k^2 \cos 2\theta_{\boldsymbol{k'}} + k'^2 \cos 2\theta_{\boldsymbol{k}} + 2kk' \cos(\theta_{\boldsymbol{k}} + \theta_{\boldsymbol{k'}})\right] \\ &+ (\delta_{\mu1}\delta_{\nu2} + \delta_{\mu2}\delta_{\nu1}) \left[k^2 \sin 2\theta_{\boldsymbol{k'}} + k'^2 \sin 2\theta_{\boldsymbol{k}} + 2kk' \sin(\theta_{\boldsymbol{k}} + \theta_{\boldsymbol{k'}})\right]. \end{aligned} \tag{17}$$

The other is the transition intra the subband $j = 2$:

$$K_{\mu\nu,22}(\boldsymbol{q}) = -\frac{g}{L^2}\sum_{ss'\boldsymbol{k}} \frac{f[\epsilon_{s2}(k)] - f[\epsilon_{s'2}(k')]}{\epsilon_{s2}(k) - \epsilon_{s'2}(k')} I_{ss',22}. \tag{18}$$

By using the fact that the subband $j = 2$ in the conduction band ($s = +1$) is empty in the weak-doped limit, it can be approximately given as

$$K_{\mu\nu,22}(\boldsymbol{q}) \approx \frac{2ge^2}{m^2L^2}\sum_{\boldsymbol{k}} \frac{1}{\epsilon_k - \epsilon_{k'}}\left[\frac{1}{2}(\boldsymbol{k}+\frac{\boldsymbol{q}}{2})^2\delta_{\mu\nu} + \frac{ss'}{8}G_{\mu\nu}\right], \tag{19}$$

with

$$\begin{aligned} G_{\mu\nu} = &(\delta_{\mu1}\delta_{\nu1} - \delta_{\mu2}\delta_{\nu2})\left[k^2\cos 2\theta_{\boldsymbol{k}} + k'^2\cos 2\theta_{\boldsymbol{k'}} + 2kk'\cos(\theta_{\boldsymbol{k}}+\theta_{\boldsymbol{k'}})\right] \\ &+(\delta_{\mu1}\delta_{\nu2} + \delta_{\mu2}\delta_{\nu1})\left[k^2\sin 2\theta_{\boldsymbol{k}} + k'^2\sin 2\theta_{\boldsymbol{k'}} + 2kk'\sin(\theta_{\boldsymbol{k}}+\theta_{\boldsymbol{k'}})\right]. \end{aligned} \tag{20}$$

From the above, we firstly obtain the analytic expression of the susceptibility of bilayer graphene at zero temperature as:

$$\chi(\boldsymbol{q};\epsilon_F) = \frac{ge^2}{8\pi m}\left\{\log\frac{2k_F^2 + \sqrt{4k_F^4+q^4}}{4\Lambda^2} + \frac{1}{3}\left[1 + (1-\frac{4k_F^2}{q^2})^{3/2}\theta(q-2k_F)\right]\right\}, \tag{21}$$

where $\theta(x)$ is the step function defined by $\theta(x) = 1(x > 0)$ and $0(x < 0)$, which is a centra result of our work. From Eq.(21), on the one hand, we can give the orbital susceptibility of BLG at zero wave number as

$$\chi(\boldsymbol{q}=0;\epsilon_F) = \frac{ge^2}{8\pi m}\left[\log\frac{\epsilon_F}{\Delta} + \frac{1}{3}\right]. \tag{22}$$

This result is same as the result given in [15, 22], which shows a logarithmically diverging behavior at $\epsilon_F = 0$. On the other hand, we can give the orbital susceptibility of BLG at zero Fermi energy as

$$\chi(\boldsymbol{q};\epsilon_F=0) = \frac{ge^2}{4\pi m}\left[\log\frac{q}{2\Lambda} + \frac{1}{3}\right]. \tag{23}$$

This also shows a logarithmically diverging behavior at $q = 0$. It is easy to see that just by replacing ϵ_F with $\gamma q/2$ and increasing the coefficient to its double times, we can transform the susceptibility $\chi(\boldsymbol{q}=0;\epsilon_F)$ into $\chi(\boldsymbol{q};\epsilon_F=0)$.

The orbital magnetic susceptibility $\chi(\boldsymbol{q})$ of bilayer graphene as a function of wave number is shown in Fig.[1]. For comparing the wave number-dependent behaviors of susceptibility of the MLG, BLG and 2DEG systems, we provide below the finite wave number susceptibility of MLG and 2DEG, which has been given in Ref.[18],

$$\chi(\boldsymbol{q};\epsilon_F) = -\frac{ge^2v}{16}\frac{1}{q}\theta(q-2k_F)\left[1 + \frac{2}{\pi}\frac{2k_F}{q}\sqrt{1-\left(\frac{2k_F}{q}\right)^2} - \frac{2}{\pi}\sin^{-1}\frac{2k_F}{q}\right] \qquad (for\ MLG), \tag{24}$$

$$\chi(\boldsymbol{q};\epsilon_F) = \frac{ge^2}{24\pi m}\left[\left(1-\frac{4k_F^2}{q^2}\right)^{3/2}\theta(q-2k_F) - 1\right] \qquad (for\ 2DEG). \tag{25}$$

At $q = 0$, the susceptibility of BLG $-\chi(0,\epsilon_F) \propto \log(\Delta/\epsilon_F)$ is rather different from that of MLG, where $-\chi(0,\epsilon_F) \propto \delta(\epsilon_F)$, and 2DEG, where $-\chi(0,\epsilon_F) \propto 1$. By comparing their diverging behaviors, it can be found that the BLG in some sense shows an intermediate behavior between the MLG and 2DEG. For small q, the $-\chi(\boldsymbol{q};\epsilon_F)$ of BLG deviates from the $-\chi(0;\epsilon_F)$ as $(q/2k_F)^4$, and falls more rapidly as q increase. On the other hand, the susceptibility of MLG vanishes while 2DEG maintains as a constant for the whole regime $q < 2k_F$ (see Fig.[1] of Ref. [18]). At $q = 2k_F$, the susceptibility $\chi(2k_F;\epsilon_F)$ of MLG and 2DEG are both constants (zero for MLG) which are independent of the Fermi wave number k_F, but for BLG, we have

$$\chi(2k_F;\epsilon_F) = \frac{ge^2}{8\pi m}\left(\log\frac{\epsilon_F}{\Delta} + \frac{1}{3} + \log\frac{1+\sqrt{5}}{2}\right), \tag{26}$$

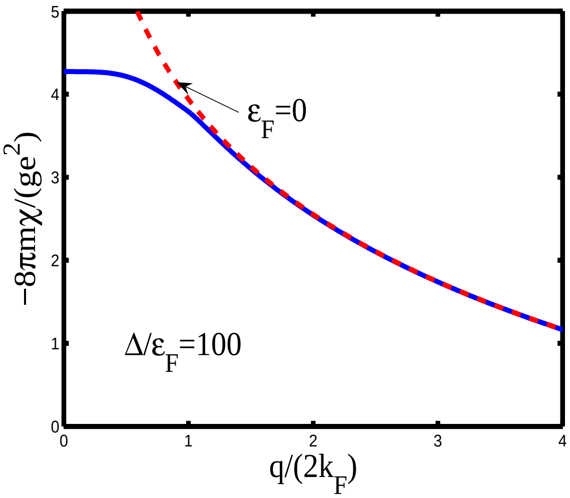

FIG. 1: Magnetic susceptibility $\chi(\boldsymbol{q})$ in bilayer graphene. Here we use $\Delta/\epsilon_F = 100$.

which is dependent of the k_F. In contrast to the MLG, the susceptibility of BLG has no singular behavior at $q = 2k_F$, and it is continuous as well as its first derivative. For large q, especially for $q \gg 2k_F$, $-\chi(q)$ of BLG rapidly approaches the curve of Eq. (23) and falls as $\log(1/q)$, very different from that of MLG where the susceptibility falls off more rapidly ($\sim 1/q$) and 2DEG where it falls as $1/q^2$. Due to having the same parabolic energy dispersion in the low energy limit, susceptibility of Bilayer graphene and 2DEG share the same term $ge^2(1-4k_F^2/q^2)^{3/2}\theta(q-2k_F)/(24\pi m)$.

4. RESPONSES TO SPECIFIC EXTERNAL MAGNETIC FIELD

Now we study the responses of bilayer graphene to different types of magnetic field. First let us consider the case of a neutral BLG (i.e., $\epsilon_F = 0$) under a sinusoidal magnetic field $\boldsymbol{B}(\boldsymbol{r}) = B_0 \cos qx \boldsymbol{e}_z$. Defining $\chi(q) \equiv \chi(\boldsymbol{q}, \epsilon_F = 0)$, we have the induced magnetization $\boldsymbol{m}(\boldsymbol{r}) = \chi(q)\boldsymbol{B}(\boldsymbol{r})$, the induced current $\boldsymbol{j}(\boldsymbol{r}) = q\chi(q)B_0 \sin qx \boldsymbol{e}_y$, and the z component of induced counter magnetic field on BLG

$$\boldsymbol{B}_{ind}(\boldsymbol{r}) = -\alpha_g(q)\boldsymbol{B}(\boldsymbol{r}), \tag{27}$$

with the magnetic field screening factor

$$\alpha_g(q) = -\frac{ge^2 q}{2m}\left[\log\frac{q}{2\Lambda} + \frac{1}{3}\right]. \tag{28}$$

When $q \to 0$, we have $\alpha_g(q) \to 0$; i.e., under a constant magnetic field there is no counter magnetic field on BLG, which is different from that of MLG. In MLG, the magnetic field screening factor is fixed and independent of q and the specific form of external field, the induced magnetic field above the graphene layer is simply equivalent to the field of a mirror image of the original object reflected with respect to the graphene layer but reduced by α_g [18]. However, this argument does not fit for the case of BLG, since the magnetic field screening factor of BLG is dependent of q and complicated.

Next we consider the case of a line current I flowing along the $+y$ direction above the BLG, and passing through the point $(0, 0, d)$ ($d > 0$). The z component of the magnetic field on BLG is $B(\boldsymbol{r}) = -2Ix/(x^2 + d^2)$. For $\epsilon_F = 0$, the induced magnetization can be given as

$$m(\boldsymbol{r}) = -\frac{Ige^2}{2\pi m}\frac{x}{x^2+d^2}\left[\log(2\Lambda\sqrt{x^2+d^2}) + \frac{d}{x}\arctan\frac{x}{d} - \gamma_E + \frac{1}{3}\right], \tag{29}$$

here $\gamma_E \approx 0.577$ is the Euler constant. By using $\boldsymbol{j}_{ind} = \nabla\times\boldsymbol{m}(\boldsymbol{r})$, we obtain the induced electric current $j_{ind}(\boldsymbol{r}) = j_y\boldsymbol{e}_y$, where

$$j_y = \frac{Ige^2}{2\pi m}\frac{1}{(x^2+d^2)^2}\left\{(d^2-x^2)\left[\log(2\Lambda\sqrt{x^2+d^2}) - \gamma_E + \frac{1}{3}\right] - 2dx\arctan\frac{x}{d} + (x^2+d^2)\right\}. \tag{30}$$

The integral of j_y in x exactly equals to 0, which means the external electric current I can not induce an effective transport electric current on the BLG, in contrast to that of MLG, where I induces an effective electric current $-\alpha_g I$. The induced magnetic field on BLG can be given as $\boldsymbol{B}_{ind}(\boldsymbol{r}) = B_z \boldsymbol{e}_z$ with

$$B_z = \frac{Ige^2}{m}\frac{1}{(x^2+d^2)^2}\left[2dx\left(\log\frac{\sqrt{x^2+d^2}}{8\Lambda d^2}+\gamma_E-\frac{1}{3}\right)+(d^2-x^2)\arctan\frac{x}{d}\right]. \tag{31}$$

In MLG, the induced magnetic field $-\alpha_g Ix/(x^2+d^2)$ is equivalent to the field created by a current $-\alpha_g I$ flowing at $z=-d$. This argument does not fit for the case of BLG as shown in Eq.(31). At large distance $x \gg d$, the induced magnetic field is proportion to $\sim 1/x^2$ comparing with $\sim 1/x$ in MLG. However, the original current is repelled by a force $\approx \alpha_g(1/2d)I^2/d$ per unit length, which can be approximately but not exactly considered as a force created by a current $\alpha_g(q)I$ at $z=-d$ with $q=1/2d$.

As another typical example, we study the the induced magnetization, electric current and magnetic field by a magnetic monopole q_m laying above the BLG. Suppose q_m is located at the point $(0,0,d)$, $(d>0)$, and the BLG plane is $z=0$. The magnetic field perpendicular to the BLG is given as $B(\boldsymbol{r}) = q_m d/(r^2+d^2)^{3/2}$ with $r=\sqrt{x^2+y^2}$. For neutral BLG, the induced magnetization is given by

$$m(\boldsymbol{r}) = -\frac{q_m g e^2}{4\pi m d^2}\left\{F(\frac{r}{d})-(\log 2\Lambda r-1/3)\left[1+(\frac{r}{d})^2\right]^{-3/2}\right\}, \tag{32}$$

where the function

$$F(x)=\frac{1}{x^2}\int_0^\infty zJ_0(z)\log z e^{-z/x}dz. \tag{33}$$

At small distance ($r \ll d$) and large distance ($r \gg d$), the induced magnetization can be written as

$$m(r)=\frac{q_m g e^2}{4\pi m}\times\begin{cases}\left\{\log 2\Lambda d+\gamma_E-\frac{4}{3}-\frac{3}{2}(r/d)^2\left[\log 2\Lambda r-\frac{1}{3}\right]\right\}/d^2 & (for \quad r\ll d)\\ 1/r^2 & (for \quad r \gg d)\end{cases} \tag{34}$$

$$\tag{35}$$

It is interesting to see that at large distance the induced magnetization of BLG $m(r) \propto 1/r^2$, while that of MLG $\propto 1/r$ and 2DEG $\propto 1/r^3$; i.e., the BLG shows a behavior as the crossover from MLG to 2DEG. The integral of $m(r)$ over the plane has a logarithmically diverging behavior $\propto \log R$ when the distance $R \to \infty$. According to Eq.(32), the corresponding electric current can be given by $\boldsymbol{j}(\boldsymbol{r}) = -(\partial m/\partial r)\boldsymbol{e}_\theta \equiv j_\theta \boldsymbol{e}_\theta$. When r is small or large, we obtain

$$j_\theta=\frac{q_m g e^2}{4\pi m}\times\begin{cases}3r\log 2\Lambda r/d^4 & (for \quad r\ll d)\\ 2/r^3 & (for \quad r\gg d)\end{cases} \tag{36}$$

$$\tag{37}$$

Remind that our results are confined to the limit $\Lambda r \gg 1$, and therefore j_r is positive through out the realistic distance. The current j_θ in MLG $\propto r/(r^2+d^2)^{3/2}$, whose asymptotic form is $\propto r$ at small distance and $\propto 1/r^2$ at large distance. We can find that the induced currents j_θ of MLG and BLG are qualitatively different in all distance. However, similar to the case of line current, the force between the monopole and the BLG can be approximately written as $\alpha_g(q)q_m^2/(2d)^2$ with $q=1/d$, which has the same form as that of MLG $\alpha_g q_m^2/(2d)^2$.

For doped bilayer graphene ($\epsilon_F \neq 0$), the corresponding response current $j_\theta(r)$ for different values of k_F are shown in Fig.[2]. We can find that the current change slightly as the Fermi wave number increase from $k_F d=0$ to $k_F d=1$; i.e., the induced current has a weak Fermi wave number dependence, which is rather different from that of MLG. This arises from the fact that the dominant term involving k_F in the susceptibility is logarithmically.

Different from the traditional 2DEG, MLG has a peculiar property [18]: (1) The counter field induced by the response current mimics a mirror image of the original object. (2) The object is repelled by a diamagnetic force from the MLG, as if there exists its mirror image with a reduced amplitude on the other side of MLG. With the investigation above, we find that argument (1) can be not extended to BLG. However, the argument (2) still be approximately correct for weak-doped BLG, and it only needs to replace the constant reduced amplitude with a reduced amplitude dependent with the typical length of the systems. The BLG, in some sense, still show an intermediate behavior between the MLG and 2DEG.

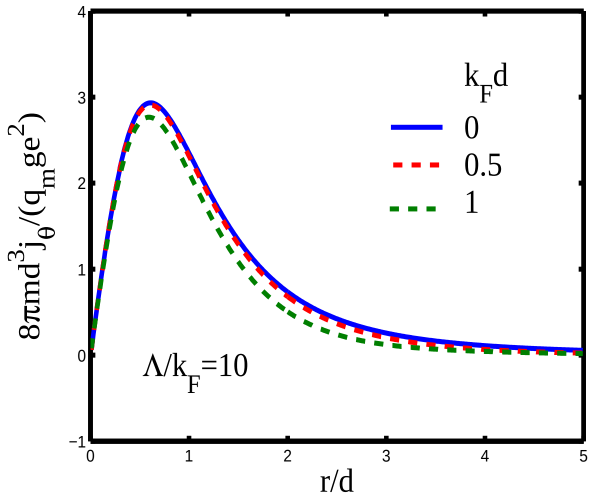

FIG. 2: Electric current $j_\theta(r)$ on bilayer graphene induced by a magnetic charge q_m at $z = d$. Here we use $\Lambda/k_F = 10$.

It is significant to compare the contribution of Landau diamagnetism to the whole magnetism with that of Pauli paramagnetism in BLG. At $\epsilon_F = 0$, the Pauli spin susceptibility $\chi^{spin}(q)$, which is given by the density-density response function [25], is equivalent to $g_v m\mu_B^2 \log 4/2\pi$, where μ_B is the Bohr magneton. With Eq.(23), we obtain the ratio $\chi^{spin}/\chi^{orb} \sim (0.03)^2/(\log 2\Lambda/q)$, which is rather small in our theory ($for\ q \ll \Lambda$).

The temperature also has an influence on the BLG diamagnetism. For $q = 0$, this has been discussed by Safran [22], who shows the susceptibility with finite temperature and Fermi energy can approximately take the form

$$\chi(\boldsymbol{q} = 0; \epsilon_F; T) \propto \log|\mu_-/\Delta| - 1 + (\mu_+/k_BT)\log|\mu_+/\mu_-| \qquad (for \quad \mu_+ \ll \Delta). \tag{38}$$

here $\mu_\pm = \epsilon_F \pm k_BT/2$. For finite q, we expect that $\chi(q)$ deviates from $\log q$ in regime $q \le \sqrt{2m|\epsilon_F - k_BT/2|}$, which means the temperature has notable affection on the diamagnetism of a neutral BLG when the typical length scale exceeds $2\pi/\sqrt{2mk_BT}$, about $70\mu m$ at $T = 1$K.

All of the above, we assume an ideal 2D BLG electron gas and ignored the distance d between up layer and bottom layer of bilayer graphene. In order to obtain an analytic expression of the susceptibility of bilayer graphene, we assume the wave number k_F and q is much smaller than the cutoff wave number Λ. An alternative farther investigation can be focused on a more general case that k_F is commensurate to or even larger than Λ.

5. CONCLUSIONS

In this article, we study analytically the orbital magnetic susceptibility of a weak-doped bilayer graphene (BLG) in spatially smoothly varying magnetic fields by the low-energy Hamiltonian and obtain the general analytic expression of the orbital susceptibility of BLG, with finite wave number and Fermi energy, at zero temperature. The induced magnetization, electric current by the nonuniform magnetic fields in BLG are studied which are different from that of MLG and 2DEG, but the argument, that the magnetic object placed above the BLG is repelled by a diamagnetic force which is equivalent to a force produced by mirror image on the other side of BLG, still be approximately hold, only by replacing the constant reduced amplitude with a reduced amplitude dependent with the typical length of the system. Logarithmically-dependent behaviors are found extensively exist in both the orbital magnetism and the induced physical quantities by specific external field. BLG shows crossover behaviors in the responses to the external magnetic field as the intermediate between MLG and 2DEG. The weak Fermi wave number dependent behaviors, as a distinctive electric property of BLG, are found in induced magnetization and electric current.

Acknowledgement

This work is supported by NSFC Grant No.10675108.

[1] E. McCann and V. I. Fal'ko, Phys. Rev. Lett. 96, 086805 (2006); J. Nilsson, A. H. Castro Neto, N. M. R. Peres, and F. Guinea, Phys. Rev. B 73, 214418 (2006); B. Partoens and F. M. Peeters, Phys. Rev. B 74, 075404 (2006); M. Koshino and T. Ando, Phys. Rev. B 73, 245403 (2006); I. Snyman and C. W. J. Beenakker, Phys. Rev. B 75, 045322 (2007).
[2] S. Morozov, K. Novoselov, M. Katsnelson, F. Schedin, D. Elias, J. Jaszczak, and A. Geim, Phys. Rev. Lett. 100, 016602 (2008).
[3] K. Novoselov *et al.*, Nature Phys. 2, 177 (2006); J. Oostinga *et al.*, Nature Mater. 7, 151 (2008).
[4] H. Min, B. Sahu, S. K. Banerjee, and A. H. MacDonald, Phys. Rev. B 75, 155115 (2007).
[5] E. McCann, Phys. Rev. B 74, 161403(R) (2006).
[6] C. L. Lu, C. P. Chang, Y. C. Huang, R. B. Chen and M. L. Lin, Phys. Rev. B 73, 144427 (2006).
[7] F. Guinea, A. H. C. Neto and N. M. R. Peres, Phys. Rev. B 73, 245426 (2006).
[8] Y. Zhang, T. T. Tang, C. Girit, Z. Hao, M. C. Martin, A. Zettl, M. F. Crommie, Y. R. Shen and F. Wang, Nature 459, 820 (2009).
[9] K. S. Krishnan, Nature 133, 174 (1934); N. Ganguli and K. S. Krishnan, Proc. R. Soc. London 177, 168 (1941).
[10] J. W. McClure, Phys. Rev. 104, 666 (1956); J. W. McClure, Phys. Rev. 119, 606 (1960).
[11] A. Ghosal, P. Goswami, and S. Chakravarty, Phys. Rev. B 75, 115123 (2007).
[12] S. G. Sharapov, V. P. Gusynin, and H. Beck, Phys. Rev. B 69, 075104 (2004).
[13] H. Fukuyama, J. Phys. Soc. Jpn. 76, 043711 (2007).
[14] M. Koshino and T. Ando, Phys. Rev. B 75, 235333 (2007).
[15] M. Koshino and T. Ando, Phys. Rev. B 76, 085425 (2007).
[16] M. Nakamura and L. Hirasawa, Phys. Rev. B 77, 045429 (2008).
[17] A. H. Castro Neto *et al.*, Rev. Mod. Phys. 81, 109 (2009).
[18] M. Koshino, Y. Arimura and T. Ando, Phys. Rev. Lett. 102, 177203 (2009).
[19] A. Principi, Marco Polini and G. Vignale, Phys. Rev. B 80, 075418 (2009).
[20] M. Koshino and T. Ando, Phys. Rev. B 81, 195431 (2010).
[21] A. Principi, Marco Polini, G. Vignale and M. I. Katsnelson, Phys. Rev. Lett. 104, 225503 (2010).
[22] S. A. Safran, Phys. Rev. B 30, 421 (1984).
[23] T. Ando, J. Phys. Soc. Jpn. 76, 104711 (2007).
[24] G. D. Mahan, *Many-Particle Physics* (Plenum, New York, 1990).
[25] E. H. Hwang and S. Das Sarma, Phys. Rev. Lett. 101, 156802 (2008).